PERGAMON

International Journal of Solids and Structures 37 (2000) 4811–4823

INTERNATIONAL JOURNAL OF SOLIDS and STRUCTURES

www.elsevier.com/locate/ijsolstr

Three-dimensional vibrations of thick spherical shell segments with variable thickness

Jae-Hoon Kang[a, 1], Arthur W. Leissa[b,*]

[a] *School of Constructional and Environmental System Engineering, Kyongju University, Kyongju, Kyongbook, South Korea*
[b] *Applied Mechanics Program, The Ohio State University, Columbus, OH, USA*

Received 28 September 1998; in revised form 20 June 1999

Abstract

A three-dimensional method of analysis is presented for determining the free vibration frequencies and mode shapes of spherical shell segments with variable thickness. Displacement components u_ϕ, u_z, and u_θ in the meridional, normal, and circumferential directions, respectively, are taken to be sinusoidal in time, periodic in θ, and algebraic polynomials in the ϕ and z directions. Potential (strain) and kinetic energies of the spherical shell segment are formulated, and upper bound values of the frequencies are obtained by minimizing the frequencies. As the degree of the polynomials is increased, frequencies converge to the exact values. Novel numerical results are presented for thick spherical shell segments with constant or linearly varying thickness and completely free boundaries. Convergence to four-digit exactitude is demonstrated for the first five frequencies of the spherical shell segments. The method is applicable to thin spherical shell segments, as well as thick and very thick ones.

Keywords: Vibration; Three-dimensional; Thick shell; Spherical shell; Shell segment; Variable thickness; Ritz method

1. Introduction

Spherical shells are extensively used in civil, mechanical, aircraft, and naval structures. The free vibration of solid and hollow spheres has been a subject of study for more than a century, sometimes with interest in the oscillations of the earth.

The problem of radial vibrations of the solid sphere was first discussed by Poisson (1829). Over 50 years later, Jaerisch (1880), Lamb (1882) and Chree (1889) considered the propagation of free harmonic waves in an elastic solid sphere. Jaerisch (1880) showed that the solution could be

* Corresponding author. Fax: +1-614-292-7369.
[1] Current address: Department of Architecture, Chung-Ang University, Seoul, South Korea.

0020-7683/00/$ - see front matter
PII: S0020-7683(99)00182-1

expressed by means of spherical harmonics. The result was obtained independently by Lamb (1882) who gave an account of the simpler modes of vibration and of the nature of the nodal division of the sphere. He used rectangular coordinates to obtain the equations governing the free vibration of the solid sphere, and Chree (1889) subsequently obtained the equations in the more convenient spherical coordinates.

The corresponding problem of a closed hollow sphere was first analyzed by Lamb (1883). Much later, the vibration of hollow spheres was also studied by Shah et al. (1969), using 2D and exact 3D theory, and natural frequency parameters for several shells with different inner to outer radius ratios were presented in graphical form. Cohen and Shah (1972) used two auxiliary variables and obtained two classes of vibrations for a spherically isotropic, hollow sphere in a vacuum on the basis of 3D elasticity theory. Three displacement functions were introduced, and then further expanded in terms of the spherical harmonics, so that the problem was finally reduced to a set of second-order ordinary differential equations. The Frobenius power series method was used to seek the solution of the equations. But the solutions they obtained were only special cases of the complete solution, and difficulty existed in locating the expressions of displacement and stress components by their method. Grigorenko and Kilina (1990) used a 3D formulation and two approximate 2D theories, the classical Kirchhoff-Love theory and a refined Timoshenko-type theory, to examine hollow thin-walled laminated spherical shells. Graphical results were presented for a hollow sphere comprised of a single, isotropic layer, and one comprised of three, orthotropic layers. Chang and Demkowicz (1995) determined natural frequencies of a vibrating hollow, elastic sphere using both the 3D elasticity and Kirchhoff shell theory. Ding and Chen (1996) studied the nonaxisymmetric free vibrations of a spherically isotropic shell embedded in an elastic medium, on the basis of 3D elasticity theory. Three displacement functions were introduced to simplify the governing equations of a spherically isotropic medium for the free vibration problem. They expressed explicitly the frequency equations considering the coupled conditions at the interface between shell and elastic medium. Jiang et al. (1996) provided numerical values for the natural frequency parameters for a significant, but not excessive, number of modes of vibration of a small selection of hollow spheres comprised of two or three layers of linear elastic, homogeneous and isotropic materials. In the paper, the 3D equations used were given for a two-layered hollow sphere as derived from the work of Sâto and Usami (1962) and Shah et al. (1969). The equations for an N-layered hollow sphere could be obtained by analogy. Two other publications that treat layered spheres are those of Nelson (1973) and Shah and Frye (1975).

The above mentioned literature uses 3D theory, and deals with solid or closed hollow spheres of constant thickness. To the authors' knowledge, there is no literature for spherical shell segments based on 3D analysis. Gautham and Ganesan (1992) reported some studies on free vibration analysis of open spherical shells, based on a thick (2D) shell theory. A thick shell finite element was developed for the analysis of general shells of revolution. Frequencies were obtained for spherical caps with and without center cutout having simply supported or clamped boundary conditions. Recently, Lim et al. (1996) analyzed the spherical shell with variable thickness using 2D shell theory. In their paper, the vibration of shallow spherical and ellipsoidal dishes with variable thickness along the gradient from the apex was studied. The Ritz method was employed and the results were compared with finite element and experimental ones.

In the present 3D analysis, the Ritz method is used to obtain accurate frequencies for thick spherical shell segments of uniform or varying thickness. Although the method itself does not yield exact solutions, proper use of displacement components in the form of algebraic polynomials permits one to obtain frequency upper bounds that are as close to the exact values as desired. Frequencies presented in this work are thus obtained that are very close to their exact values, being exact to four significant figures.

2. Analysis

Fig. 1 shows the cross-section of a spherical segment with thickness (h) varying in the meridional direction (ϕ) and having a midsurface spherical radius a. The ends of the shell (top and bottom) are determined by ϕ_t and ϕ_b, where the thicknesses are h_t and h_b, respectively. The curvilinear coordinate system (ϕ, z, θ), also shown in the figure, is used in the analysis. The meridional (ϕ) and thickness (z) coordinates are measured from the axis of revolution (y) and normally from the midsurface of the shell, respectively, and θ is the circumferential angle.

Utilizing tensor analysis in the first author's dissertation (Kang, 1997), the three equations of motion in the curvilinear coordinate system (ϕ, z, θ) were found to be:

$$\sigma_{\phi z,\,z}+\frac{1}{a+z}\left[(\sigma_{\phi\phi}-\sigma_{\theta\theta})\cot\phi+\sigma_{\phi\theta,\,\theta}\csc\phi+\sigma_{\phi\phi,\,\phi}+3\sigma_{\phi z}\right]=\rho\ddot{u}_{\phi},$$

$$\sigma_{zz,\,z}+\frac{1}{a+z}\left[\sigma_{\phi z}\cot\phi+\sigma_{z\theta,\,\theta}\csc\phi+\sigma_{\phi z,\,\phi}-\sigma_{\theta\theta}+2\sigma_{zz}\right]=\rho\ddot{u}_{z},$$

$$\sigma_{z\theta,\,z}+\frac{1}{a+z}\left[2\sigma_{\phi\theta}\cot\phi+\sigma_{\theta\theta,\,\theta}\csc\phi+\sigma_{\phi\theta,\,\phi}+3\sigma_{z\theta}\right]=\rho\ddot{u}_{\theta}, \tag{1}$$

where the σ_{ij} are the normal ($i=j$) and shear ($i\neq j$) stress components; u_ϕ, u_z, and u_θ are the displacement components in the ϕ, z, and θ directions, respectively; ρ is mass density per unit volume; the commas indicate spatial derivatives; and the dots denote time derivatives.

The well-known relationships between the stress and tensorial strains ε_{ij} of isotropic, linear elasticity are:

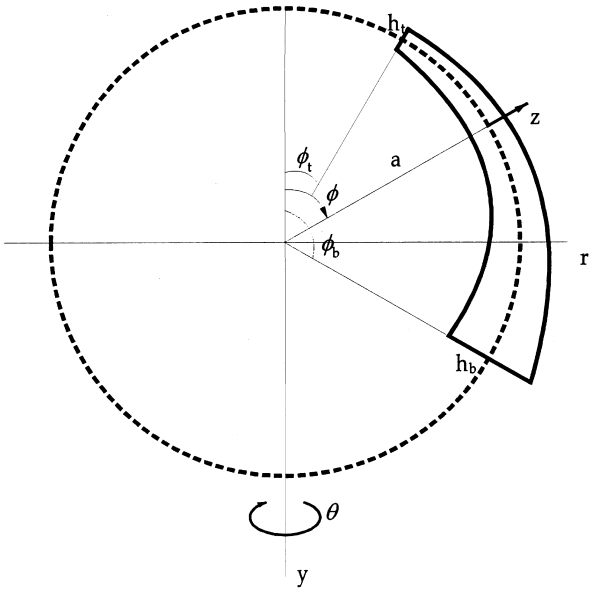

Fig. 1. Cross-section of a spherical shell segment with varying thickness and the coordinate system (ϕ, z, θ).

$$\sigma_{ii} = \lambda(\varepsilon_{\phi\phi} + \varepsilon_{zz} + \varepsilon_{\theta\theta}) + 2G\varepsilon_{ii}, \tag{2a}$$

$$\sigma_{ij} = 2G\varepsilon_{ij}, \quad i \neq j, \tag{2b}$$

where λ and G are the Lamé parameters, expressed in terms of Young's modulus (E) and Poisson's ratio (ν) for an isotropic solid as:

$$\lambda = \frac{E\nu}{(1+\nu)(1-2\nu)}, \qquad G = \frac{E}{2(1+\nu)}. \tag{3}$$

The 3D tensorial strains are found to be related to the three displacements u_ϕ, u_z, and u_θ, by (Kang, 1997)

$$\varepsilon_{\phi\phi} = \frac{1}{a+z}(u_{\phi,\,\phi} + u_z),$$

$$\varepsilon_{zz} = u_{z,\,z},$$

$$\varepsilon_{\theta\theta} = \frac{1}{(a+z)\sin\phi}\left(u_{\theta,\,\theta} + u_\phi\cos\phi + u_z\sin\phi\right),$$

$$\varepsilon_{\phi z} = \frac{1}{2}\left[u_{\phi,\,z} - \frac{1}{a+z}(u_\phi - u_{z,\,\phi})\right],$$

$$\varepsilon_{\phi\theta} = \frac{1}{2(a+z)}\left[u_{\theta,\,\phi} + \frac{1}{\sin\phi}\left(u_{\phi,\,\theta} - u_\theta\cos\phi\right)\right],$$

$$\varepsilon_{z\theta} = \frac{1}{2}\left[u_{\theta,\,z} + \frac{1}{(a+z)\sin\phi}\left(u_{z,\,\theta} - u_\theta\sin\phi\right)\right]. \tag{4}$$

Substituting Eqs. (2a) and (2b) into Eq. (1), one obtains a set of second-order partial differential equations in u_ϕ, u_z, and u_θ governing free vibrations. Exact solutions are intractable, however, because of the variable coefficients, $1/(a+z)$, $1/(a+z)\sin\phi$, and $1/(a+z)^2\sin\phi$, that appear in many terms. Alternatively, one may approach the problem from an energy perspective.

Because the strains are related to the displacement components by Eq. (4), and the stresses are linearly related to the strains, unacceptable strain and stress singularities may be encountered at $\phi = 0$ and π due to the term $1/(a+z)\sin\phi$. The present analysis is limited to open spherical shell segments. That is, ϕ_t and ϕ_b are neither zero nor π. Closed shells occur if either ϕ_t or $\phi_b = 0$ or π. Such cases require the enforcement of regularity conditions at each junction where the shell closed.

During vibratory deformation of the body, its strain (potential) energy (V) is the integral over the domain (Ω):

$$V = \frac{1}{2}\int_\Omega \left(\sigma_{\phi\phi}\varepsilon_{\phi\phi} + \sigma_{zz}\varepsilon_{zz} + \sigma_{\theta\theta}\varepsilon_{\theta\theta} + 2\sigma_{\phi z}\varepsilon_{\phi z} + 2\sigma_{\phi\theta}\varepsilon_{\phi\theta} + 2\sigma_{z\theta}\varepsilon_{z\theta}\right)(a+z)^2\sin\phi\,\mathrm{d}\phi\,\mathrm{d}z\,\mathrm{d}\theta. \tag{5}$$

Substituting Eqs. (2a) and (2b) into Eq. (5) results in the strain energy in terms of the three displacements:

$$V = \frac{1}{2}\int_{\Omega}\left[\lambda(\varepsilon_{\phi\phi}+\varepsilon_{zz}+\varepsilon_{\theta\theta})^2+2G\left\{\varepsilon_{\phi\phi}^2+\varepsilon_{zz}^2+\varepsilon_{\theta\theta}^2+2\left(\varepsilon_{\phi z}^2+\varepsilon_{z\theta}^2+\varepsilon_{\phi\theta}^2\right)\right\}\right](a+z)^2\sin\phi\,\mathrm{d}\phi\,\mathrm{d}z\,\mathrm{d}\theta, \tag{6}$$

where the tensorial strains ε_{ij} are defined in terms of the three displacements by Eq. (4).

The kinetic energy (T) is simply

$$T = \frac{1}{2}\int_{\Omega}\rho\left(\dot{u}_{\phi}^2+\dot{u}_z^2+\dot{u}_{\theta}^2\right)(a+z)^2\sin\phi\,\mathrm{d}\phi\,\mathrm{d}z\,\mathrm{d}\theta. \tag{7}$$

For convenience, the thickness coordinate z is made dimensionless as:

$$\zeta \equiv \frac{z}{h_{\mathrm{m}}}, \tag{8}$$

where h_{m} is the average shell thickness. If the thickness varies linearly, it is defined by

$$h_{\mathrm{m}} \equiv \frac{h_{\mathrm{t}}+h_{\mathrm{b}}}{2}. \tag{9}$$

For the free, undamped vibration, the time (t) response of the three displacements is sinusoidal and, moreover, the circular symmetry of the shell allows the displacements to be expressed by

$$u_{\phi}(\phi,\zeta,\theta,t) = U_{\phi}(\phi,\zeta)\cos n\theta\,\sin(\omega t+\alpha), \tag{10a}$$

$$u_z(\phi,\zeta,\theta,t) = U_z(\phi,\zeta)\cos n\theta\,\sin(\omega t+\alpha), \tag{10b}$$

$$u_{\theta}(\phi,\zeta,\theta,t) = U_{\theta}(\phi,\zeta)\sin n\theta\,\sin(\omega t+\alpha), \tag{10c}$$

where U_{ϕ}, U_z, and U_{θ} are displacement functions of ϕ and ζ, ω is a natural frequency, and α is an arbitrary phase angle determined by the initial conditions. The circumferential wave number is taken to be an integer ($n = 0,\ 1,\ 2,\ 3,\ldots,\ \infty$) for a circumferentially closed shell ($0 \le \theta \le 360^{\circ}$), to ensure periodicity in θ. Then Eqs. (10a)–(10c) account for all free vibration modes except for the torsional ones. These modes arise from an alternative set of solutions which are the same as Eqs. (10a)–(10c), except that $\cos n\theta$ and $\sin n\theta$ are interchanged. For $n > 0$, this set duplicates the solutions of Eqs. (10a)–(10c), with the symmetry axes of the mode shapes being rotated. But for $n = 0$ the alternative set reduces to $u_{\phi} = u_z = 0$, $u_{\theta} = U_{\theta}^{*}(\phi,\ z)\sin(\omega t+\alpha)$, which corresponds to the torsional modes. The displacements uncouple by circumferential mode number (n), leaving only coupling in ϕ and z.

The Ritz method uses the maximum potential (strain) energy ($V_{\max}$) and the maximum kinetic energy ($T_{\max}$) functionals in a cycle of vibratory motion. The functionals are obtained by setting $\sin^2(\omega t+\alpha)$ and $\cos^2(\omega t+\alpha)$ equal to unity in Eqs. (6) and (7) after the displacements (10a)–(10c) are substituted, and by using the nondimensional thickness coordinate ζ as follows:

$$V_{\max} = \frac{h_{\mathrm{m}}G}{2}\int_{\phi_{\mathrm{t}}}^{\phi_{\mathrm{b}}}\int_{-\delta(\phi)/2}^{\delta(\phi)/2}\left[\left\{\frac{\lambda}{G}(K_1+K_2+K_3)^2+2\left(K_1^{\,2}+K_2^{\,2}+K_3^{\,2}\right)+K_4^{\,2}\right\}\Gamma_1+\left(K_5^{\,2}+K_6^{\,2}\right)\Gamma_2\right]$$
$$\times\,(a/h_{\mathrm{m}}+\zeta)^2\sin\phi\,\mathrm{d}\zeta\,\mathrm{d}\phi, \tag{11}$$

$$T_{\max} = \frac{\rho h_{\mathrm{m}}^3}{2}\int_{\phi_{\mathrm{t}}}^{\phi_{\mathrm{b}}}\int_{-\delta(\phi)/2}^{\delta(\phi)/2}\left[\left(U_{\phi}^{\,2}+U_z^{\,2}\right)\Gamma_1+U_{\theta}^{\,2}\Gamma_2\right](a/h_{\mathrm{m}}+\zeta)^2\sin\phi\,\mathrm{d}\zeta\,\mathrm{d}\phi, \tag{12}$$

where

$$K_1 \equiv \frac{U_\phi \cos\phi + U_z \sin\phi + nU_\theta}{(a/h_m + \zeta)\sin\phi}, \tag{13a}$$

$$K_2 \equiv \frac{U_z + U_{\phi,\phi}}{a/h_m + \zeta}, \tag{13b}$$

$$K_3 \equiv U_{z,\zeta}, \tag{13c}$$

$$K_4 \equiv \frac{U_\phi - U_{z,\phi}}{a/h_m + \zeta} - U_{\phi,\zeta}, \tag{13d}$$

$$K_5 \equiv \frac{nU_z + U_\theta \sin\phi}{(a/h_m + \zeta)\sin\phi} - U_{\theta,\zeta}, \tag{13e}$$

$$K_6 \equiv \frac{1}{a/h_m + \zeta}\left[U_{\theta,\phi} - \frac{nU_\phi + U_\theta \cos\phi}{\sin\phi}\right]. \tag{13f}$$

Assuming that the shell thickness variation is limited to be linear with ϕ, the nondimensional thickness $\delta(\phi)$ can be defined by

$$\delta(\phi) \equiv \frac{h(\phi)}{h_m} = \frac{1}{1-\phi^*}\left(\frac{1-h^*}{\phi_m}\phi + h^* - \phi^*\right), \tag{14}$$

where

$$\phi_m \equiv \frac{\phi_t + \phi_b}{2}, \tag{15}$$

h^* and ϕ^* are the thickness and meridional angle ratios, defined by

$$h^* \equiv \frac{h_t}{h_m}, \qquad \phi^* \equiv \frac{\phi_t}{\phi_m}, \tag{16}$$

and Γ_1 and Γ_2 are constants defined by

$$\Gamma_1 \equiv \int_0^{2\pi} \cos^2 n\theta \, d\theta = \begin{cases} 2\pi & \text{if } n = 0 \\ \pi & \text{if } n \geq 1 \end{cases},$$

$$\Gamma_2 \equiv \int_0^{2\pi} \sin^2 n\theta \, d\theta = \begin{cases} 0 & \text{if } n = 0 \\ \pi & \text{if } n \geq 1 \end{cases}. \tag{17}$$

It is known that λ and G have the same units as E from Eq. (3). The nondimensional constant λ/G in Eq. (11) involves only ν; i.e., $\lambda/G = 2\nu/(1-2\nu)$.

The displacement functions U_ϕ, U_z, and U_θ in Eqs. (10a)–(10c) are further assumed as

$$U_\phi(\phi,\zeta)=\eta_\phi(\phi,\zeta)\sum_{i=0}^{I}\sum_{j=0}^{J}A_{ij}\phi^i\zeta^j, \tag{18a}$$

$$U_z(\phi,\zeta)=\eta_z(\phi,\zeta)\sum_{k=0}^{K}\sum_{l=0}^{L}B_{kl}\phi^k\zeta^l, \tag{18b}$$

$$U_\theta(\phi,\zeta)=\eta_\theta(\phi,\zeta)\sum_{m=0}^{M}\sum_{n=0}^{N}C_{mn}\phi^m\zeta^n, \tag{18c}$$

and similarly for U_θ^*, where i, j, k, l, m, and n are integers; I, J, K, L, M, and N are the highest degrees of the polynomial terms; A_{ij},B_{kl}, and C_{mn} are arbitrary coefficients; and the η are functions depending upon the geometric boundary conditions to be enforced. For example:

1. Completely free: $\eta_\phi=\eta_z=\eta_\theta=1$,
2. Top end ($\phi=\phi_t$) fixed, remaining boundaries free: $\eta_\phi=\eta_z=\eta_\theta=\phi-\phi_t$,
3. Bottom end ($\phi=\phi_b$) fixed, remaining boundaries free: $\eta_\phi=\eta_z=\eta_\theta=\phi-\phi_b$,
4. Both ends fixed, remaining boundaries free: $\eta_\phi=\eta_z=\eta_\theta=(\phi-\phi_t)(\phi-\phi_b)$,
5. Inner surface ($z=-h/2$) fixed, remaining boundaries free: $\eta_\phi=\eta_z=\eta_\theta=\zeta+\delta(\phi)/2$,
6. Outer surface ($z=h/2$) fixed, remaining boundaries free: $\eta_\phi=\eta_z=\eta_\theta=\zeta-\delta(\phi)/2$,
7. Both surfaces restrained normally and meridionally, but not circumferentially:

$$\eta_\phi=\eta_z=\big[\zeta+\delta(\phi)/2\big]\big[\zeta-\delta(\phi)/2\big],\quad \eta_\theta=1,$$

8. Both surfaces restrained normally, but not tangentially:

$$\eta_z=\big[\zeta+\delta(\phi)/2\big]\big[\zeta-\delta(\phi)/2\big],\quad \eta_\phi=\eta_\theta=1.$$

The functions of η_ϕ, η_z, and η_θ shown above, impose only the necessary geometric constraints. Together with the algebraic polynomials in Eqs. (18a)–(18c), they form function sets which are mathematically complete (Kantorovich and Krylov, 1958, pp. 266–268). Thus, the function sets are capable of representing any 3D motion of the body with increasing accuracy as the indices $I, J, \ldots, N$ are increased. In the limit, as sufficient terms are taken, all internal kinematic constraints vanish, and the functions (18a)–(18c) will approach the exact solution as closely as desired.

The eigenvalue problem is formulated by minimizing the free vibration frequencies with respect to the arbitrary coefficients, thereby minimizing the effects of the internal constraints present, when the function sets are finite. This corresponds to the equations (Ritz, 1909):

$$\frac{\partial}{\partial A_{ij}}(V_{\max}-T_{\max})=0\quad (i=0,1,2,\ldots,I;\ j=0,1,2,\ldots,J),$$

$$\frac{\partial}{\partial B_{kl}}(V_{\max}-T_{\max})=0\quad (k=0,1,2,\ldots,K;\ l=0,1,2,\ldots,L),$$

$$\frac{\partial}{\partial C_{mn}}(V_{\max}-T_{\max})=0\quad (m=0,1,2,\ldots,M;\ n=0,1,2,\ldots,N). \tag{19}$$

Eq. (19) yield a set of $(I+1)(J+1)+(K+1)(L+1)+(M+1)(N+1)$ linear, homogeneous, algebraic

equations in the unknowns A_{ij}, B_{kl}, and C_{mn}. For a nontrivial solution, the determinant of the coefficient matrix is set equal to zero, which yields the frequencies (eigenvalues). These frequencies are upper bounds on the exact values. The mode shape (eigenfunction) corresponding to each frequency is obtained, in the usual manner, by substituting each ω back into the set of algebraic equations, and solving for the ratios of coefficients.

3. Convergence study

Table 1 shows a convergence study made for a completely free, thick ($h_m/a = 0.2$) spherical shell segment ($\phi_t = 30^\circ$, $\phi_b = 90^\circ$) with considerable thickness variation ($h_t/h_b = 1/3$). The second shape in Fig. 2 is drawn with these ratios. Poisson's ratio (ν) is taken to be 0.3. Table 1 shows the first five nondimensional frequencies $\omega a\sqrt{\rho/G}$ for one circumferential wave ($n = 1$) in the mode shapes. The number of polynomial terms taken in the thickness (z or ζ) direction is

Table 1
Convergence of frequencies $\omega a\sqrt{\rho/G}$ of a completely free, spherical shell segment with linearly varying thickness for the five lowest modes of $n = 1$ with $\phi_t = 30^\circ$, $\phi_b = 90^\circ$, $h_m/a = 0.2$, $h_t/h_b = 1/3$, and $\nu = 0.3$

TZ[a]	TP[b]	DET[c]	1	2	3	4	5
2	**2**	**12**	2.478	2.897	5.024	6.664	13.536
2	**4**	**24**	2.022	2.447	2.973	4.510	5.658
2	**6**	**36**	2.011	2.441	2.914	4.464	5.186
2	**8**	**48**	2.010	2.441	2.912	4.456	5.085
2	**10**	**60**	2.009	2.441	2.911	4.456	5.081
3	**2**	**18**	2.476	2.887	5.015	6.611	13.053
3	**4**	**36**	2.001	2.435	2.903	4.499	5.623
3	**6**	**54**	1.989	2.429	2.848	4.422	4.963
3	**8**	**72**	1.987	2.429	2.846	4.404	4.872
3	**10**	**90**	1.987	2.429	2.845	4.403	4.869
4	**2**	**24**	2.475	2.885	5.014	6.603	12.429
4	**4**	**48**	1.997	2.434	2.895	4.494	5.614
4	**6**	**72**	1.985	2.428	2.840	4.410	4.918
4	**8**	**96**	1.983	2.427	2.838	4.388	4.832
4	**10**	**120**	1.982	2.427	2.837	4.387	4.829
5	**2**	**30**	2.474	2.882	5.013	6.597	12.427
5	**4**	**60**	1.997	2.433	2.894	4.494	5.611
5	**6**	**90**	1.984	2.428	2.839	4.409	4.914
5	**8**	**120**	1.983	2.427	2.837	4.387	4.830
5	**10**	**150**	1.982	2.427	2.837	4.386	4.827
6	**2**	**36**	2.474	2.881	5.013	6.596	12.424
6	**4**	**72**	1.996	2.433	2.893	4.493	5.609
6	**6**	**108**	1.984	2.428	2.839	4.408	4.912
6	**8**	**144**	1.982	2.427	2.837	4.387	4.829
6	**9**	**162**	1.982	2.427	2.837	4.386	4.827

[a] Total number of natural polynomial terms used in the z or ζ direction.
[b] Total number of natural polynomial terms used in the ϕ direction.
[c] Determinant order.

$TZ = J + 1 = L + 1 = N + 1$, and the number in the meridional (ϕ) direction is $TP = I + 1 = K + 1 = M + 1$. The resulting order of the frequency determinant generated, is labeled "DET" in Table 1.

It is seen that the frequencies have converged monotonically to four significant figures in Table 1 and, for the reasons given above, these are exact values to four digits. Values underlined are the converged values for the smallest determinant sizes with which they are achieved. The four-digit convergence for the first five frequencies requires determinants of order 96–150. For $TZ = 6$, the largest value of TP which may be used is nine, before numerical ill-conditioning is encountered with the ordinary algebraic polynomial trial functions of Eqs. (18a)–(18c).

It is interesting to note that the solutions presented in Table 1 for $TZ = 2$, by which a thick (2D) shell theory is represented, even when $TP = 10$, are inaccurate when compared with the converged values for higher TZ. Nevertheless, these relatively inaccurate solutions are much more accurate than would be obtained from classical (thin) shell theory, and also more accurate than solutions from a first order shear deformation theory. The latter theory corresponds to $J = N = 1$, but L is only zero, preventing thickness-stretch displacement. The classical theory has additional kinematic constraints between U_ϕ, U_z, and U_θ. Conversely, even if three-digit accuracy is needed for the frequencies, then Table 1 shows that TZ must be at least four. Very similar convergence rates were found for the $n = 0$ (axisymmetric and torsional) and $n = 2$ modes.

Extensive additional convergence studies were also made (Kang, 1997) for $n = 0$ (axisymmetric and torsional) for the spherical shell segment of Table 1, as well as for spherical shell segments having other

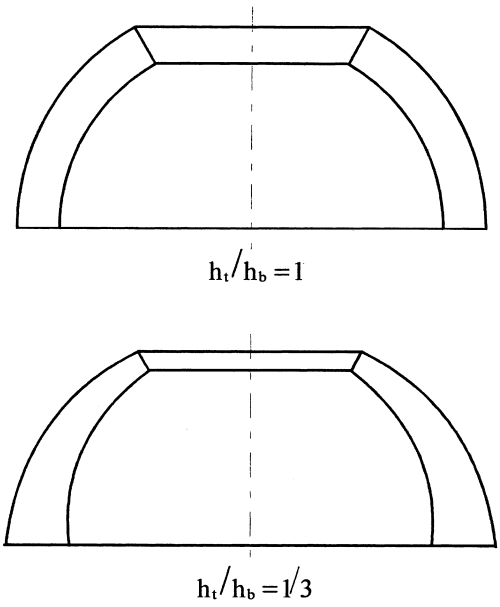

Fig. 2. Cross-sections of spherical shell segments for $\phi_t = 30°$, $\phi_b = 90°$, and $h_m/a = 0.2$.

thickness variations ($h_t/h_b = 1$ and 0). Convergence rates for all cases were approximately the same as that seen in Table 1.

4. Numerical results and discussion

Tables 2 and 3 present accurate (four significant figure) nondimensional frequencies $\omega a\sqrt{\rho/G}$ of completely free, thick ($h_m/a = 0.2$) spherical shell segments for $(\phi_t, \phi_b) = (30^\circ, 90^\circ)$ (see Fig. 2), (45°,

Table 2
Nondimensional frequencies $\omega a\sqrt{\rho/G}$ of completely free, spherical shell segments with constant thickness ($h_t/h_b = 1$) for $h_m/a = 0.2$ and $\nu = 0.3$[a]

n	Mode	(ϕ_t, ϕ_b)				
		(30°, 90°)	(45°, 90°)	(30°, 150°)	(45°, 135°)	(30°, 120°)
0(*T*)	**1**	3.448	4.238	1.987	2.397	2.466
	2	6.241	8.072	3.386	4.238	4.303
	3	9.115	11.96	4.787	6.140	6.192
	4	12.03	15.86	6.216	8.079	8.121
	5	14.97	15.90	7.671	10.04	10.08
0(*A*)	**1**	(3) 1.879	(3) 1.653	(4) 1.672	(2) 1.468	(3) 1.705
	2	2.132	2.343	1.879	1.837	(5) 1.891
	3	2.727	3.489	2.079	2.310	2.328
	4	4.708	6.802	2.486	3.016	3.034
	5	5.520	7.010	2.969	3.778	3.829
1	**1**	(5) 2.064	2.233	(3) 1.570	(4) 1.778	(4) 1.764
	2	2.357	2.531	(5) 1.693	1.874	1.925
	3	2.919	3.593	2.332	2.607	2.579
	4	4.310	4.760	2.407	2.909	2.983
	5	4.886	6.813	3.157	3.477	3.585
2	**1**	2.608	2.754	1.709	1.980	2.016
	2	2.815	3.455	2.110	2.237	2.279
	3	3.799	4.048	2.685	3.209	3.278
	4	4.987	5.883	2.835	3.285	3.336
	5	5.285	6.657	3.583	4.404	4.262
3	**1**	(2) 1.539	(2) 0.8263	(1) 1.098	(1) 0.7473	(2) 1.498
	2	3.304	3.323	(2) 1.490	2.234	2.398
	3	3.333	4.028	2.110	2.851	2.916
	4	4.880	5.175	2.710	3.651	3.741
	5	5.487	6.736	3.318	3.861	4.054
4	**1**	(1) 0.8948	(1) 0.7451	2.108	(3) 1.767	(1) 1.245
	2	2.739	(4) 1.844	2.602	(5) 1.873	2.367
	3	4.102	4.054	3.135	2.751	3.219
	4	4.195	4.551	3.647	3.597	3.770
	5	5.766	6.177	4.227	4.316	4.439
5	**1**	(4) 1.901	(5) 1.888	2.732	2.601	2.217
	2	3.723	3.011	3.451	2.968	3.079
	3	4.970	4.898	4.191	3.565	4.090
	4	5.326	5.179	4.851	4.411	4.769
	5	6.706	6.916	5.232	5.181	5.342

[a] *Note*: *T* Torsional mode; *A* Axisymmetric mode. Numbers in parentheses identify frequency sequences.

90°), (30°, 150°), (45°, 135°) (see Fig. 3), and (30°, 120°), with constant thickness ($h_t/h_b = 1$, Table 2) and considerable thickness variation ($h_t/h_b = 1/3$, Table 3). Poisson's ratio (ν) was taken to be 0.3.

Thirty-five frequencies are given for each configuration, which arise from seven circumferential mode numbers (n) (i.e., $n = 0(T)$, $0(A)$, 1, 2, 3, 4, 5) and the first five modes for each value of n, where T and A indicate torsional and axisymmetric modes, respectively. Numbers in parentheses identify the first five frequencies for each configuration. The zero frequencies of rigid body modes are omitted from the tables.

It is seen that irrespective of the values of (ϕ_t, ϕ_b), the fundamental (lowest) frequencies for constant

Table 3
Nondimensional frequencies $\omega a\sqrt{\rho/G}$ of completely free, spherical shell segments with linearly varying thickness ($h_t/h_b = 1/3$) for $h_m/a = 0.2$ and $\nu = 0.3$[a]

n	Mode	(ϕ_t, ϕ_b)				
		(30°, 90°)	(45°, 90°)	(30°, 150°)	(45°, 135°)	(30°, 120°)
0(*T*)	**1**	3.668	4.475	2.132	2.470	2.580
	2	6.385	8.192	3.492	4.290	4.394
	3	9.200	11.94	4.862	6.172	6.255
	4	11.91	12.29	6.268	8.093	8.160
	5	12.11	15.80	7.707	10.04	10.10
0(*A*)	**1**	(3) 1.809	(4) 1.634	(2) 0.8571	(3) 1.438	(3) 1.654
	2	(5) 2.163	2.383	1.764	1.832	1.878
	3	2.688	3.453	1.911	2.300	2.303
	4	4.617	6.675	2.162	2.970	2.983
	5	5.700	7.260	2.513	3.810	3.849
1	**1**	(4) 1.982	2.205	(3) 1.539	(4) 1.669	(2) 1.631
	2	2.427	2.548	1.817	1.957	2.035
	3	2.837	3.540	2.384	2.595	2.528
	4	4.386	4.966	2.465	2.881	2.940
	5	4.827	6.736	3.128	3.490	3.620
2	**1**	2.380	2.715	(4) 1.634	(5) 1.828	(5) 1.801
	2	2.916	3.440	2.196	2.340	2.383
	3	3.707	3.944	2.658	3.131	3.164
	4	4.903	6.043	2.941	3.343	3.382
	5	5.403	6.827	3.553	4.366	4.273
3	**1**	(1) 1.060	(1) 0.6925	(1) 0.7705	(1) 1.041	(1) 0.9023
	2	2.896	3.197	(5) 1.722	2.108	2.154
	3	3.464	4.011	2.137	2.875	2.912
	4	4.880	5.087	2.714	3.579	3.629
	5	5.355	6.952	3.298	3.918	4.029
4	**1**	(2) 1.250	(2) 0.8703	1.928	(2) 1.095	(4) 1.658
	2	2.273	(3) 1.484	2.385	2.140	2.052
	3	3.590	3.803	3.034	2.672	2.792
	4	4.220	4.570	3.669	3.525	3.611
	5	5.925	6.211	4.146	4.269	4.279
5	**1**	2.274	(5) 2.175	2.625	2.088	2.611
	2	3.389	2.480	3.227	2.916	2.985
	3	4.458	4.494	3.885	3.594	3.682
	4	5.114	5.266	4.639	4.285	4.441
	5	6.668	7.065	5.205	5.120	5.081

[a] *Note*: *T* Torsional mode; *A* Axisymmetric mode. Numbers in parentheses identify frequency sequences.

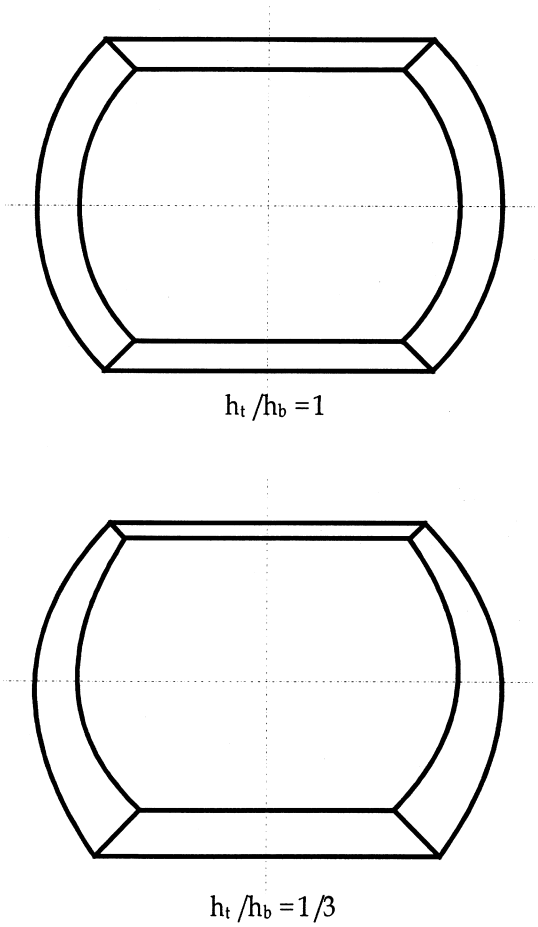

Fig. 3. Cross-sections of spherical shell segments for $\phi_t = 45°$, $\phi_b = 135°$, and $h_m/a = 0.2$

thickness are for modes having four circumferential half-waves ($n = 4$), except for $(\phi_t, \phi_b) = (30°, 150°)$ and $(45°, 135°)$ while the ones for variable thickness are for $n = 3$ with no exceptions.

The axisymmetric (''breathing'') modes are seen to be significant for each of the shell configurations, each having at least one such mode among the first five. However, the torsional modes all correspond to higher frequencies.

5. Conclusions

Accurate frequency data determined by the 3D Ritz analysis have been presented for thick, spherical shell segments. The analysis uses the 3D equations of the theory of elasticity in their general forms for isotropic, homogeneous materials. They are only limited to small strains. No other constraints are placed upon the displacements. This is in stark contrast with the classical 2D shell theories, which make very limiting assumptions about the displacement variations through the shell thickness. Although the method has the capability of analyzing accurately very thick shells which 2D shell theories (thin or

thick) cannot, it can also be applied to thin shells, thereby determining conclusively the accuracies of the shell theories.

The method is straightforward, but it is capable of determining frequencies and mode shapes as close to the exact ones as desired. It can therefore obtain benchmark results against which 3D finite element results may be compared to determine the accuracy of the latter. Moreover, the frequency determinants required by the present method are at least an order of magnitude smaller than those needed by a finite element analysis of comparable accuracy.

References

Chang, Y.-C., Demkowicz, L., 1995. Vibrations of a spherical shell: comparison of 3D elasticity and Kirchhoff shell theory. Comp. Assited Mech. Eng. Sci 2 (3), 187–206.

Chree, C., 1889. The equations of an isotropic elastic solid in polar and cylindrical coordinates, their solutions and application. Trans. Cambridge Philos. Soc. Math. Phys. Sci 14, 250–269.

Cohen, H., Shah, A.H., 1972. Free vibrations of a spherically isotropic hollow sphere. Acustica 26, 329–340.

Ding, H., Chen, W., 1996. Nonaxisymmetric free vibrations of a spherically isotropic spherical shell embedded in an elastic medium. Int. J. Solids Struct 33 (18), 2575–2590.

Gautham, B.P., Ganesan, N., 1992. Free vibration analysis of thick spherical shells. Computers and Structures 45 (2), 307–313.

Grigorenko, Y.M., Kilina, T.N., 1990. Analysis of the frequencies and modes of natural vibration of laminated hollow sphere in two- and three-dimensional formulations. Soviet Applied Mechanics 25 (12), 1165–1171.

Jaerisch, P., 1880. Journal of Mathematics (Crelle) Bd. 88.

Jiang, H., Young, P.G., Dickinson, S.M., 1996. Natural frequencies of vibration of layered hollow spheres using exact three-dimensional elasticity equations. Journal of Sound and Vibration 195 (1), 155–162.

Kang, J.H., 1997. Three-dimensional vibration analysis of thick shells of revolution with arbitrary curvature and variable thickness. Ph.D. Dissertation, Ohio State University.

Kantorovich, L.V., Krylov, V.I., 1958. Approximate Methods of Higher Analysis. Noordhoff, Groningen.

Lamb, H., 1882. Proceedings, London Mathematical Society 13, 189–212.

Lamb, H., 1883. Proceedings, London Mathematical Society 14, 50–56.

Lim, C.W., Kitipornchai, S., Liew, K.M., 1996. Modeling the vibration of a variable thickness ellipsoidal dish with central point clamp or concentric surface clamp. J. Acoust. Soc. Am 99 (1), 362–372.

Nelson, R.B., 1973. Natural vibrations of laminated orthotropic spheres. International Journal of Solids and Structures 9, 305–311.

Poisson, S.D., 1829. Mémoire sur l'équilibre et le mouvement des corps élastiques. Mémoires de l'Académie des Sciences. Paris, 8.

Ritz, W., 1909. Über eine neue methode zur lösung gewisser variationsprobleme der mathematischen physik. Journal für die Reine und Angewandte Mathematik 135, 1–61.

Sâto, Y., Usami, T., 1962. Basic study on the oscillation of a homogeneous elastic sphere. Part II: Distribution of displacement. Geophysics Magazine 31, 25–47.

Shah, A.H., Frye, M.J., 1975. Free vibrations of isotropic layered spheres. Acustica 32, 291–299.

Shah, A.H., Ramkrishnan, C.V., Datta, S.K., 1969. Three-dimensional and shell theory analysis of elastic waves in a hollow sphere. Analytical foundation. Transactions of the American Society of Mechanical Engineers, Journal of Applied Mechanics 36, 431–444.